International Journal of Engineering and Technical Research (IJETR)
ISSN: 2321-0869 (O) 2454-4698 (P), Volume-3, Issue-8, August 2015

An investigation of the durability of air cured concretes containing metakaolin

A. S. Marinos, M. S. Katsiotis, S. M. Alhassan, J. L. Gallias, M. Beazi-Katsioti

Abstract— **Metakaolin is a promising pozzolanic material which is currently used for producing high performance, high strength, lightweight cement. In this work, the effect of partially substituting cement with metakaolin on durability has been studied. Two types of cement (CEM I & II) were used with up to 20% substitution by metakaolin. Compressive strength and chloride permeability were determined at 28, 90, 180 and 360 days of hydration and carbonation depth was determined at different CO_2 exposure periods. Chloride permeability for specimens treated underwater was also determined, and a correlation with electrical conductivity was established. Experimental results show that the addition of metakaolin in cement leads to improving strength and durability. For both types of cement, 10% substitution by metakaolin resulted in decreased chloride permeability and increased compressive strength. At higher substitution ratios chloride permeability further reduces, at the expense of compressive strength. Finally, very good correlation is observed between non-steady state diffusion coefficient and electrical conductivity and between non-steady state diffusion coefficient and the initially measured current.**

Index Terms—**Air curing, Chlorides, Compressive strength, Durability.**

I. INTRODUCTION

Concrete is the most used material for building construction because of its relative low cost and its ability to form various structural shapes with great strength and durability. Environmental conditions can affect –sometimes critically- concrete service life [1]. Marine (or sea-side) environment is a typical example of a harsh environment with damaging effects for concrete structures. Chloride ions, typically found at high concentration in seashore environment, can penetrate concrete through its porous system, corrode the reinforcement and cause structural deterioration, decreasing the service life significantly [2-5].

In order to protect concrete structures from such harsh environmental conditions, stronger and less porous concrete has been developed by using high-range water-reducing admixtures and substituting clinker (the main binder of Ordinary Portland Cement - OPC) with supplementary cementitious materials like fly ash and silica fume known for their pozzolanic and filling properties [6-10]. Substitution materials which have lower Particle Size Distribution (PSD) than OPC increases binder packing density. This leads to improving concrete strength, dimensional stability and durability, thus contributing significantly to concrete service life [11-16].

Metakaolin (MK) is a promising material that can be used successfully as a supplemental cementitious material in concrete. Metakaolin is an ultrafine artificial pozzolana, produced by calcining kaolinite clay at temperatures ranging from 700 to 900°C, at which the chemically bound water is removed and the crystalline structure transforms to that of a dehydroxylated amorphous aluminosilicate constituted of lamellar particles. Various studies show that adding metakaolin in concrete as cement replacement influences mechanical and durability properties favorably [3, 9, 11, 17-21]. Metakaolin is well known to increase cement strength and improve sorptivity, while it can have an impact on chloride penetration [22].

The purpose of the present study is to determine the influence of partial cement replacement with metakaolin on mechanical strength, chloride permeability, electrical conductivity and carbonation depth of microconcretes cured up to 360 days under room conditions (T: 19 – 23°C, %RH: 55 – 70%). Micrococoncrete simulates the structure and the properties of concrete, containing only sand as aggregate. For selected mixtures, specimens were cured in water for up to 90 days, and the results were compared to air-cured specimens.

II. MATERIALS & METHODS

A. Materials

Two commercially available cements, CEM I 52.5N and CEM II / B – M (P-W) 42.5N, were used for the production of microconcrete mixtures. A commercially available Metakaolin (ARGICAL M-1000) was used as a supplementary cementitious material. Properties of the raw materials are presented in Tables I and II. Fig. 1 presents the Particle Size Distribution (PSD) of the raw materials, which was defined with Static Light Scattering (SLS) method at room temperature with a CILAS 1064 Particle Size Analyzer. Sand produced from crushed calcareous stone was used as aggregate. Chemical analysis and specific gravity are presented in Table 3, while particle size distribution determined according to ASTM C 136- 06 is shown in Fig. 2. Potable water was used for casting all microconcrete specimens, as per EN 1008 specifications [23]. A chloride free, polycarboxylate based superplasticizer (Viscocrete® 300) was employed to achieve the desired workability.

Table I. Composition and mechanical properties of CEM I 52.5 and CEM II/B – M (P-W) 42.5.

Apostolos S. Marinos, School of Chemical Engineering, National Technical University of Athens, Athens, Greece.
Marios S. Katsiotis, Department of Chemical Engineering, The Petroleum Institute, Abu Dhabi, United Arab Emirates, +97126075225.
Saeed M. Alhassan, Department of Chemical Engineering, The Petroleum Institute, Abu Dhabi, United Arab Emirates, +97126075225.
Jean-Louis Gallias, Département Génie Civil, Université de Cergy-Pontoise, Paris, France, +33134256910.
Margarita Beazi-Katsioti, School of Chemical Engineering, National Technical University of Athens, Athens, Greece.

	CEM I 52.5N	CEM II 42.5N
	%	%
SiO_2	20.93	22.1
Al_2O_3	5.8	6.27
Fe_2O_3	3.51	3.55
CaO	60.07	55.97
MgO	2.03	2.2
K_2O	0.67	0.71
Na_2O	0.2	0.3
SO_3	2.99	3.1
TiO_2	0.3	0.31
LOI	3.3	5.23
Blaine (cm^2/g)	**4176**	**4461**
Sp. Gravity (g/cm^3)	**3.06**	**2.96**
Compressive Strength		
1 day (MPa)	31.1	28.9
7 days (MPa)	43.2	40.4
28 days (MPa)	57.3	50.7

Table II. Chemical and physical properties of metakaolin.

	%
SiO_2	58.56
Al_2O_3	35.48
Fe_2O_3	1.22
CaO	0.00
MgO	0.17
K_2O	0.57
Na_2O	0.03
SO_3	0.00
TiO_2	2.16
LOI	1.31
Sp. Gravity(g/cm^3)	2.57
Blaine (cm^2/g)	20208

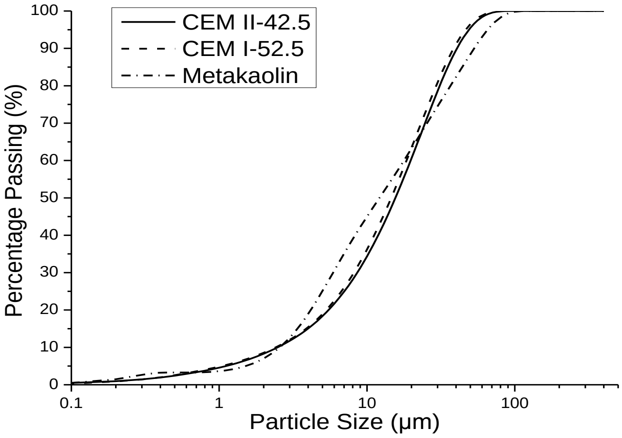

Figure 1. Particle Size Distribution of cement and metakaolin raw materials.

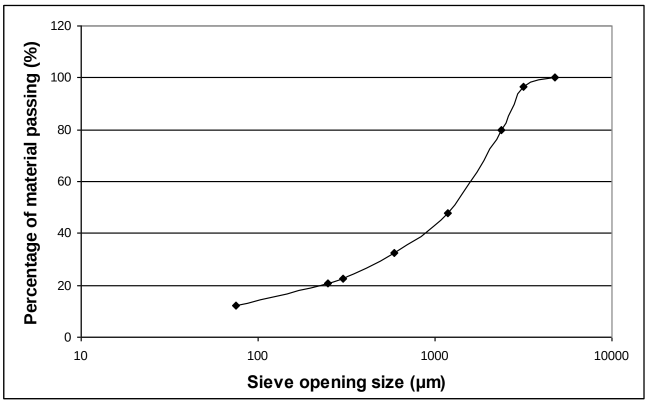

Figure 2. Particle size distribution of sand

Table 3. Chemical and physical properties of sand.

	%
SiO_2	0.00
Al_2O_3	0.00
Fe_2O_3	0.02
CaO	55.50
MgO	0.72
K_2O	0.01
Na_2O	0.00
SO_3	0.00
TiO_2	0.00
LOI	43.52
Sp. Gravity (g/cm^3)	2.7

B. Sample preparation

Five different microconcrete mixtures were designed and prepared in this study. Two of them were the control mixtures (reference), including only CEM I 52.5N and CEM II / B – M (P-W) 42.5N respectively. The remaining three mixtures included CEM II / B – M (P-W) 42.5 N partially replaced with 10% and 20% MK (by weight) and CEM I 52.5N partially replaced with 10% MK (by weight) respectively.

Table IV. Composition of microconcrete mixtures in Kg/m^3.

MIX	**A**	**B**	**C**	**D**	**E**
Binder	**CEM I 52.5**	**CEM I 52.5 + 10% MK**	**CEM II 42.5**	**CEM II 42.5 + 10% MK**	**CEM II 42.5 + 20% MK**
Cement	500	450	492	441	393
Metakaolin (MK)	0	50	0	49	98
Water	250	250	246	245	246
Sand	1502	1502	1478	1472	1474
Superplasticizer	2	5	2	4	6
AIRCON (%)	2.8	3.5	3.8	3.7	3.1
Flow Table (mm)	183	179	182	185	184

All mixtures were prepared with water to binder ratio (w/b) equal to 0.5 by weight; approximately 9L were prepared for each sample. Initially the dry materials were mixed together at low mixer speed and then water containing superplasticiser was added. Microconcrete mixture design is presented in Table IV for all samples.

Air content and flow table spreading of the fresh microconcrete were measured according to EN 459-2 and EN 1015-3:1999 respectively. Superplasticiser was added in order to keep flow table values in the range 180 ± 5mm for all mixtures.

Prismatic specimens with dimensions 40 x 40 x 160 mm and cylindrical specimens with dimensions Φ100mm x 200mm were cast for each mixture. Prismatic specimens were cast according to EN 196 – 1. Cylindrical specimens were cast in PVC moulds and compacted with a vibrating table. After casting, the cylindrical specimens were covered with a wet blanket to minimize water evaporation and cured under laboratory conditions while prismatic specimens were covered with a plastic sheet and cured in a humidity chamber. After 24 h, all specimens were demoulded and cured under room conditions (T: 19 – 23^{o}C, RH: 55 – 70%); specimens were collected at 28, 90, 180 and 360 days. These curing conditions were selected to emulate warm climates. In addition, cylindrical and prismatic specimens from C, D and E mixtures were cured at 20^{o}C in a Ca(OH)$_2$ saturated aqueous solution for 28 and 90 days.

C. Compressive strength measurements

The 40 x 40 x 160 mm specimens were used for compressive strength measurements. Compressive strength was determined according to EN 196-1. For each mixture and at each hydration age, three specimens were tested and the mean value of these measurements is reported below.

D. Non-steady state chloride coefficient (NT Build 492) measurements.

Two 50mm-thick discs were collected from the central part of each cylinder. Following, the discs were prepared according to NT Build 492 standard procedure for non-steady state chloride migration coefficient measurement [4, 24-26]. Finally, the discs were placed in the system presented in Fig. 3A, in order to conduct the measurement. The schematics on the principle of measuring with NT Build 492 are presented in Fig. 3B.

Due to the applied electrical field on each disc, chloride ions migrated from the catholyte (NaCl solution) to the analyte (NaOH solution) through the specimen. The voltage applied to each specimen and the duration of the measurement was defined by the standard. After each measurement the discs were split axially and sprayed with 0.1M AgNO$_3$ solution. AgNO$_3$ reacts with chlorides and produce AgCl, a white precipitate. The production of AgCl indicates the depth that chloride ions migrate up to a concentration of about 0.07N into the specimen porosities, as shown in Fig. 4.

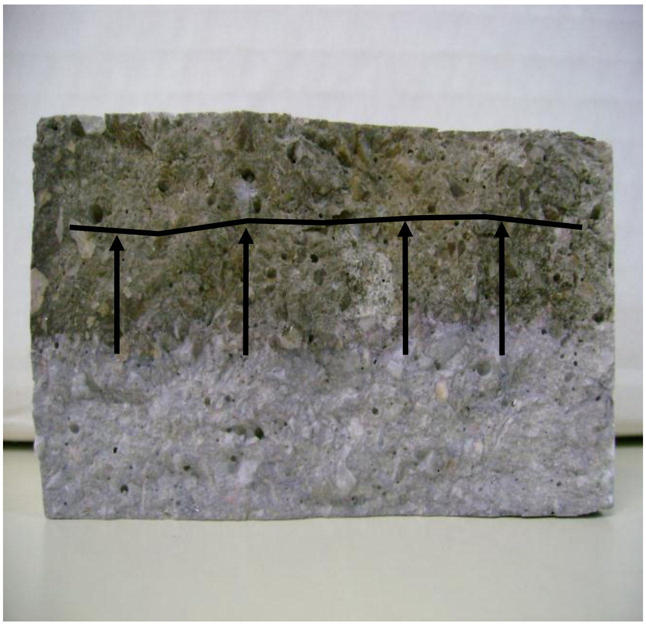

Figure 4. Depth of chloride ions migration

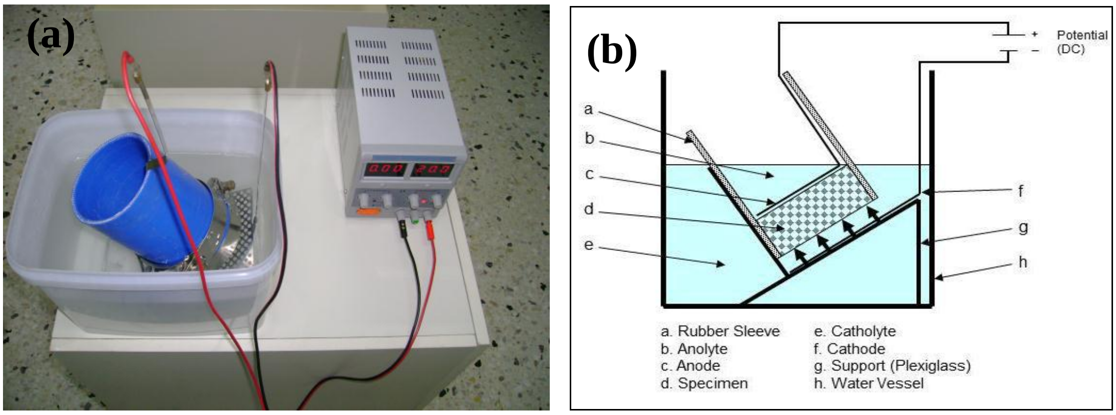

Figure 3. (a): Apparatus for non- steady state migration coefficient measurements according to NT Build 492; (b): Principle of operation for NT Build 492.

For each age and mixture two discs were tested, and the non-steady state migration coefficient (D_{nssm}) was calculated according to (1); the mean value of the migration coefficients is reported below.

$$D_{nssm} = \frac{RT}{zFE} * \frac{x_d - a\sqrt{x_d}}{t} \quad (1)$$

In Eq. (1):

- $E = \frac{U-2}{L}$
- $a = 2\sqrt{\frac{RT}{zFE}} * erf^{-1}\left(1 - \frac{2c_d}{c_0}\right)$

where:
D_{nssm}: Non-steady state migration coefficient (m^2/sec)
z: Absolute value of ion valence, for chloride, $z = 1$
F: Faraday constant, $F = 9.648 \times 10^4$ J/(V*mol)
U: Absolute value of the applied voltage, V
R: Gas constant, $R = 8.314$ J/(K*mol)
T: Average value of the Initial and Final Temperatures in the anolyte solution, K
L: Thickness of the specimen, m
x_d: Average value of the penetration depths, m
t: Test duration, seconds
erf^{-1}: Inverse of error function
c_d: Chloride concentration at which the colour changes (about 0.07N)
c_0: Chloride concentration in the catholyte solution (about 2N)

E. Accelerated carbonation testing

After curing under laboratory conditions for 5 days, two cylinders of each mixture were placed in a chamber with controlled concentration of CO_2 (22 - 23%), at temperature of 21-23°C and relative humidity 55–70%. The bottom and top surface of the specimens were sealed in order for CO_2 to penetrate through the cylinder peripheral area. After specific CO_2 exposure periods, a 20mm width slice was cut from each cylinder and the carbonation depth was determined by means of phenolphthalein indicator (Fig. 5).

III. RESULTS AND DISCUSSION

A. Compressive strength results

Fig. 6 shows the effect of metakaolin addition as cement replacement on the compressive strength for various ages.
It is obvious from Fig. 6 that the use of metakaolin as cement substitute enhances the compressive strength of microconcrete for both types of cement for up to 10% substitution at all curing ages. This can be attributed to the pozzolanic activity and improved packing of the particles that influences cement paste initial porosity. For mixtures B and D, the binder PSD is lower than in mixtures A and C, due to metakaolin addition. This results in increased packing density and hence greater compressive strength when compared to specimens with low binder PSD. Mixture E exhibits the lowest compressive strength at all ages. Two possible reasons may provide explanation of this result. The first reason is that the amount of calcium hydroxide available in the binder may be insufficient to develop new hydration products particularly calcium silicate hydrate (C-S-H) which is responsible for cement paste's strength. The second reason may be the air curing of the specimens eliminating necessary for hydration water and restricting pozzolanic activity of the binder.

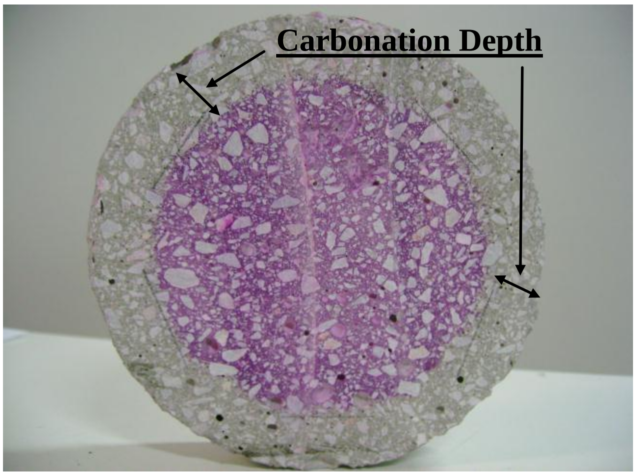

Figure 5. Carbonation depth determination using phenolphthalein.

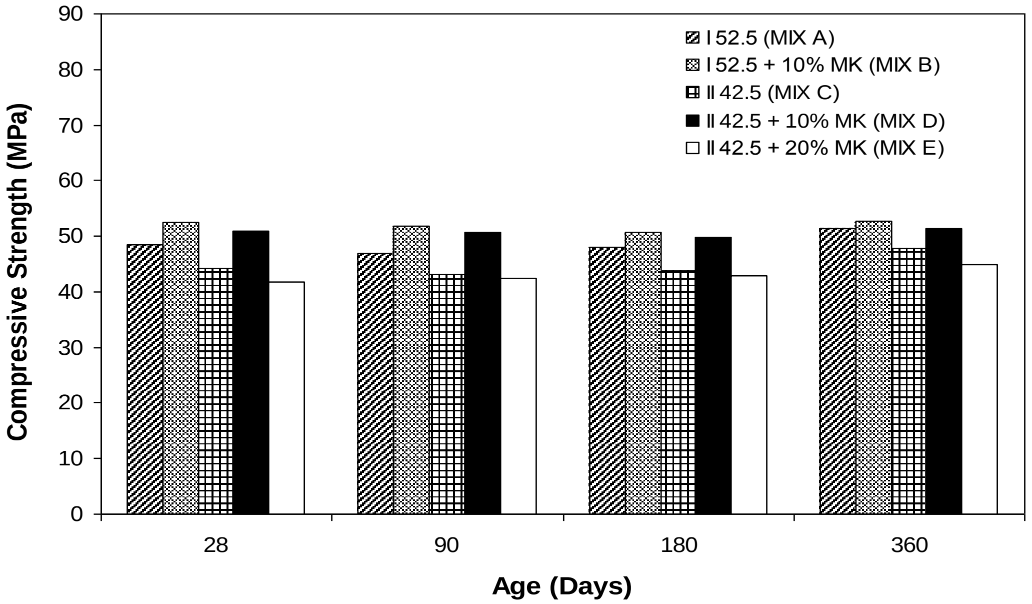

Figure 6. Compressive strength measurement results at various curing ages.

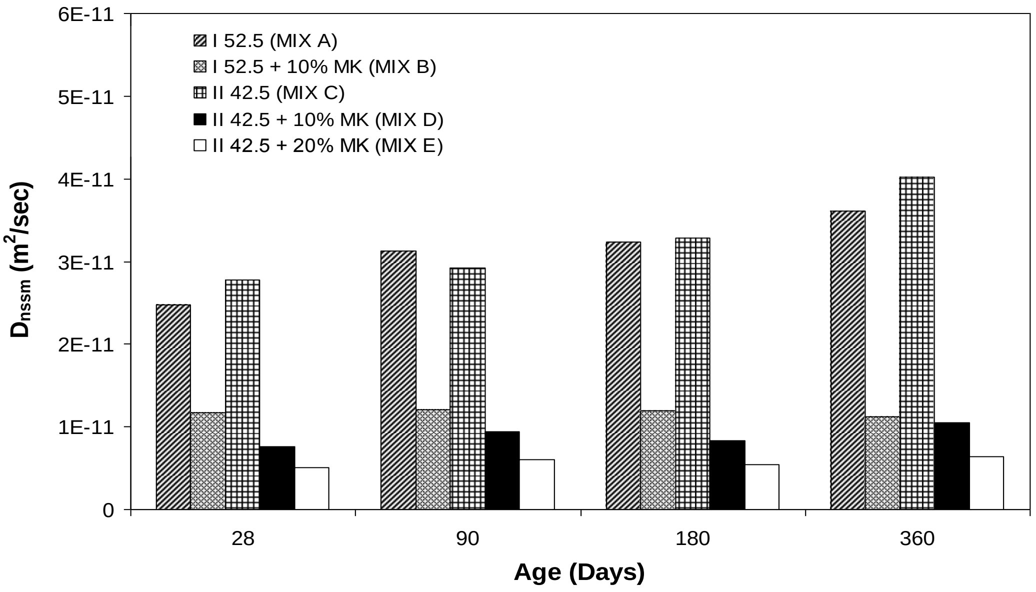

Figure 7. Non-steady state migration coefficient values at various curing ages.

Therefore the strength improvement in time for mixture E was limited. Lower clinker content (<80%) in CEM II 42.5 and air curing conditions are also the reasons behind the lower compressive strength values of mixtures C and D.

B. Non-steady state migration coefficient (D_{nssm}) results

Fig. 7 shows the effect of metakaolin addition as cement replacement on microconcrete's chloride permeability for various ages. As presented in Fig. 7, chloride permeability of the microconcretes containing metakaolin is substantially lower than those of the specimens without metakaolin for both types of cement. Specifically, mixtures D and E show three and five times respectively lower migration coefficient than mixture C at 28 days. Also, mixture B shows almost two times lower migration coefficient than mixture A at 28 days. For curing longer than 28 days, the values of the migration coefficients of mixtures B, D and E remain almost without change in time while the values of the migration coefficients of reference mixtures A and C increase, making the difference of migration coefficients values between mixtures with and without metakaolin higher.

These results show that the pozzolanic and filling properties of metakaolin lead to significant decrease of chloride permeability, thus improving concrete durability against chloride ions penetration. Furthermore, as shown in Fig. 7, mixture D exhibited slightly lower migration coefficient than mixture B. This can be attributed to the existence of fine pozzolanic materials in CEM II 42.5 such as fly ash; these materials associate with metakaolin leading to the formation of a denser microstructure with lower cement paste porosity and permeability. Finally, the mixture containing CEM II 42.5 + 20%MK (mixture E) exhibited the lowest migration coefficient of all the mixtures. Increased presence of fine pozzolanic materials in the binder (Natural Pozzolana, Fly Ash, 20% Metakaolin) promoted –under the given conditions- the formation of a complex and dense paste microstructure, thus reducing porosity and chloride permeability.

On the other hand, the progressive increasing of the migration coefficient values of reference mixtures without metakaolin with age shows that air curing of specimens damages the microstructure of these mixtures probably causing micro-cracking. The addition of metakaolin in the mixture prevent against this damage.

C. Correlation between D_{nssm} and electrical conductivity

It has been reported in literature that electrical conductivity (σ) measurements can be used as a rapid and non-destructive method for estimation of chloride permeability in concrete [27-30]. The electrical conductivity of a concrete specimen can be calculated from.(2):

$$\sigma = \frac{I_0 * L}{A * V} \qquad (2)$$

where σ = conductivity (S/m), I_0 = initial current (Ampere), L = specimen's thickness (m), V = applied voltage (Volts) and A = exposure area (m^2). In this study, the electrical conductivity was calculated from NT Build 492 experiments, setting A equal to the cylinder base surface ($0.00785 m^2$), L equal to the thickness of the specimen (50 ± 1mm); voltage was set at 30V (Initial Voltage according NT Build 492) and I_0 was the initial current that was recorded when 30 Volts were applied.

It is observed for all the air-cured specimens a high correlation between electrical conductivity and D_{nssm} and between Initial Current and D_{nssm} (Fig. 8 and 9 respectively).

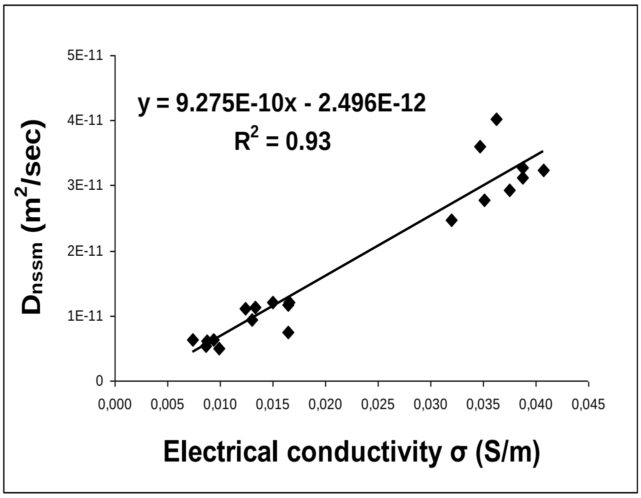

Electrical conductivity (σ) can be defined as the inverse of electrical resistivity (ρ) (Equation 3):

$$\sigma = \frac{1}{\rho} \qquad (3)$$

which can be measured in situ with Wenner method [31]. The strong correlation between electrical resistivity and D_{nssm} is shown in Fig. 10.

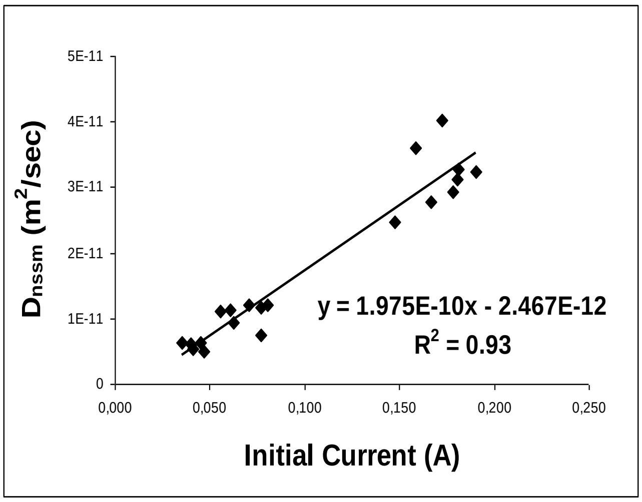

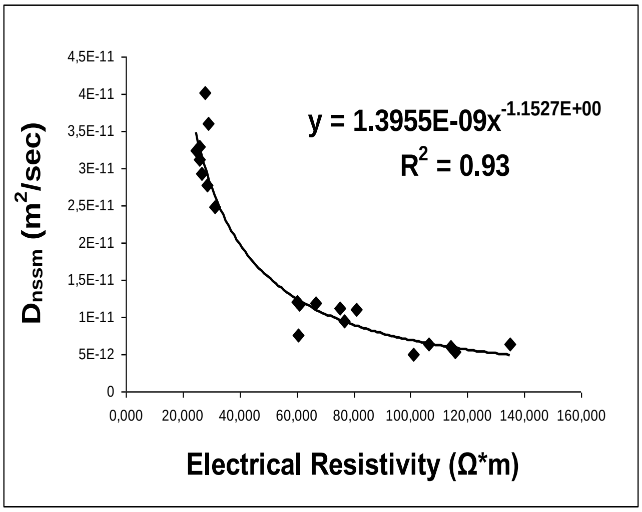

D. Influence of curing conditions on non-steady state migration coefficient and compressive strength

Fig. 11 shows the non-steady state migration coefficient of air-cured and water-cured specimens at the age of 28 and 90 days. Water-cured specimens showed lower permeability than air-cured specimens, as was expected. Higher available humidity in water-cured specimens promoted hydration reactions and lead to the formation of higher amount of hydration products than in air-cured specimens; thus a denser cement matrix was produced under water curing.

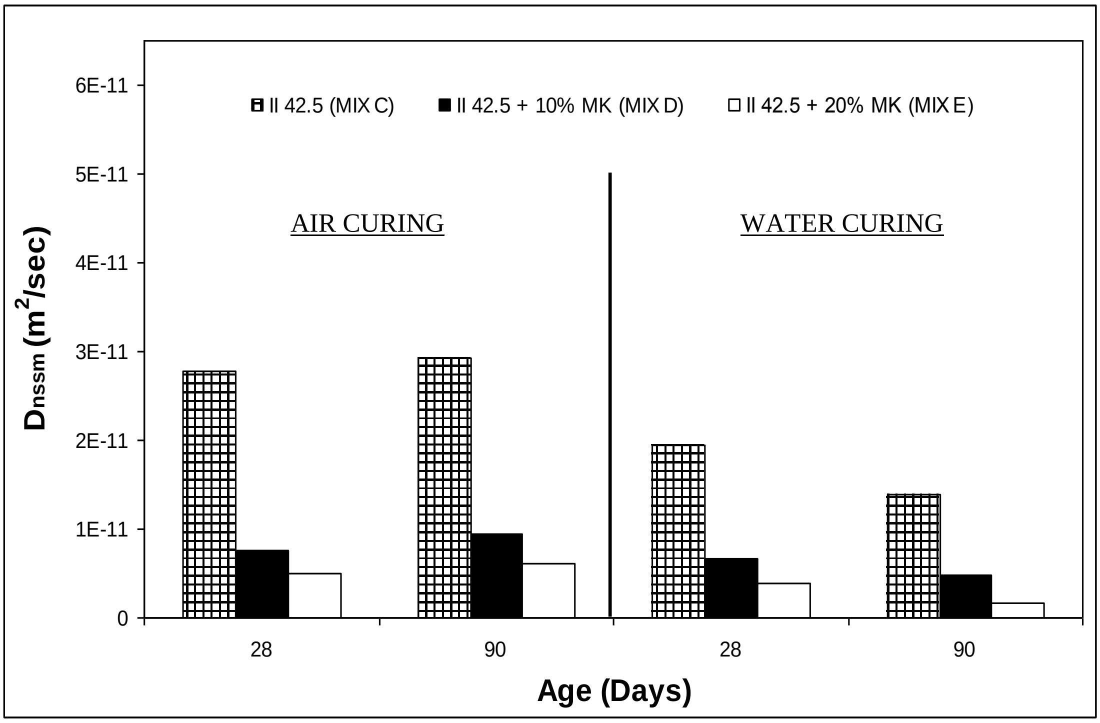

Figure 11. Non-steady state migration coefficient with age for air-cured and water-cured specimens.

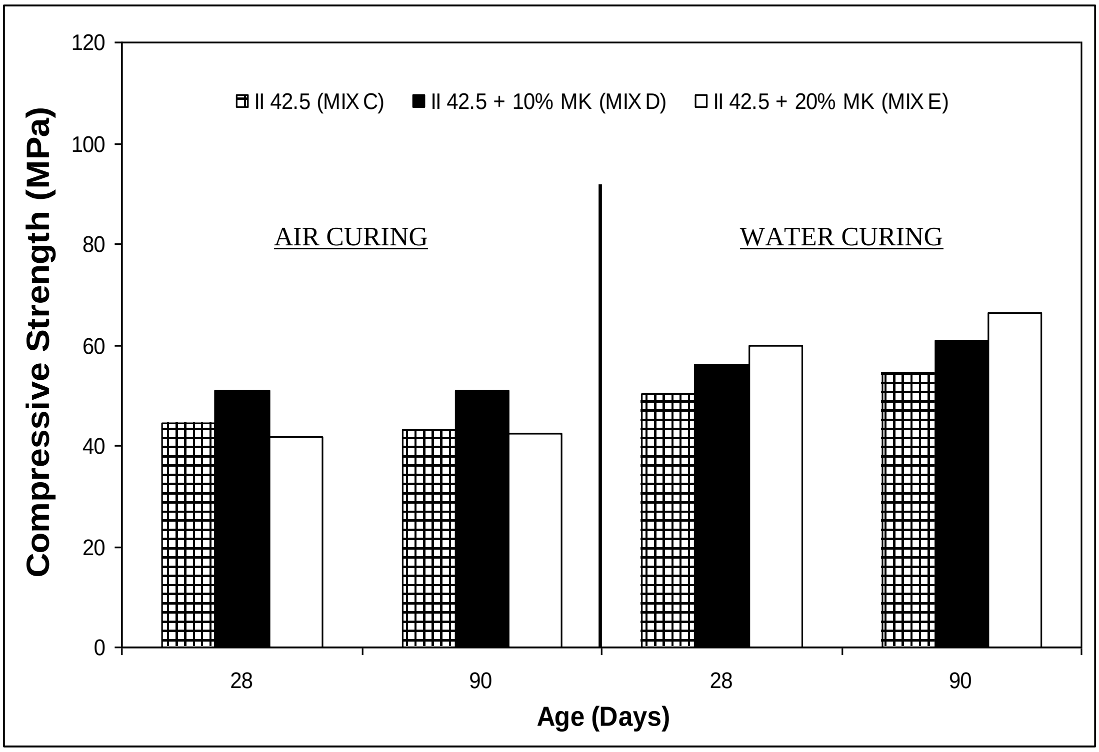

Figure 12. Compressive strength with age for water-cured and air-cured specimens.

This resulted in lower permeability and higher strength (as shown in Fig. 12). Furthermore, concerning the effect of metakaolin in cement, it is clearly shown it can lead to substantial increase of the strength of microconcrete and its durability against chloride ions penetration. The beneficial properties of metakaolin are more evident under water curing, this being the result of enhanced pozzolanic behaviour.

E. Accelerated carbonation results

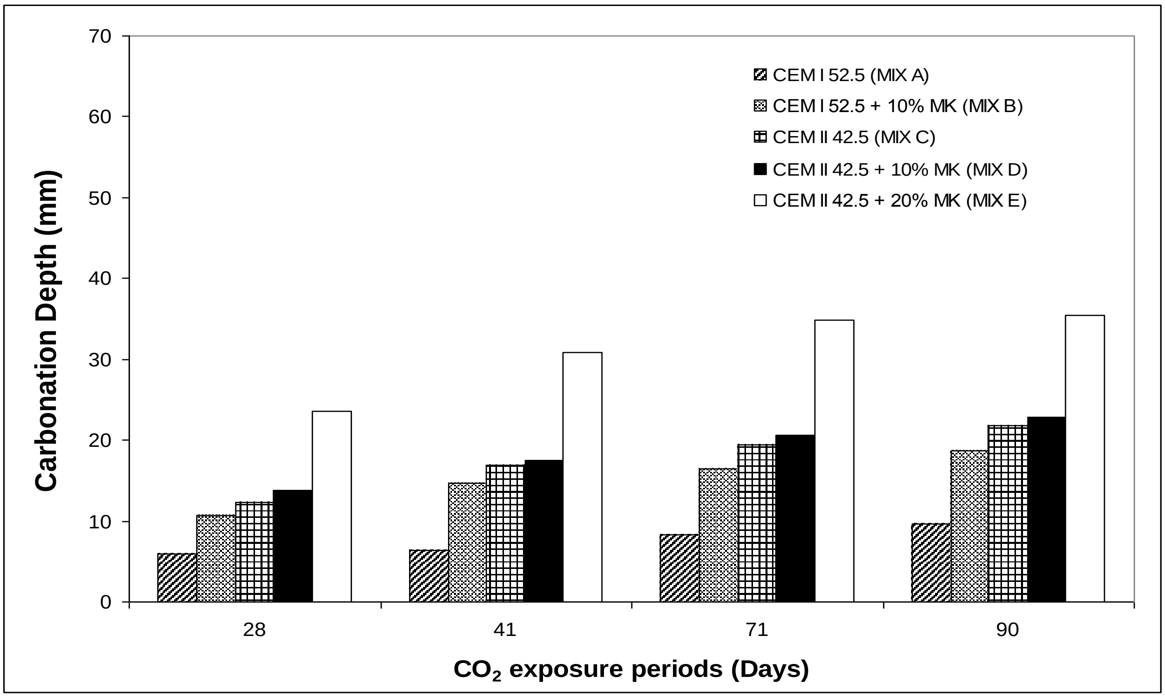

Figure 13 Carbonation depth measurements

The replacement of clinker with pozzolanic materials leads to greater carbonation of cement paste. Mix A showed the lowest carbonation depth, while mix E, exhibited the highest carbonation depth, as expected due to its higher content of pozzolanic materials in the binder (>30%). It can be concluded that the carbonation depths of concretes containing binders with pozzolanic materials are substantially greater compared with concretes containing OPC. This can be also attributed to the decrease of $Ca(OH)_2$ content due to clinker's high replacement levels and to pozzolanic reaction.

IV. CONCLUSIONS

- The use of metakaolin as cement's replacement increases microconcrete's compressive strength when the substitution is limited at 10% independently of the type of cement and the curing conditions.
- For higher than 10% substitution of cement by metakaolin, increased compressive strength is observed only for water-cured specimens; curing in water allows enhanced metakaolin pozzolanic activity. Otherwise, compressive strength is reduced for air-cured microconcrete mixtures because of poorer hydration of cement and consequently limited pozzolanic activity.
- The use of metakaolin as cement replacement decreases chloride permeability substantially for both types of cement at the curing conditions used in this study.
- The strong correlation between non-steady state migration coefficient and electrical conductivity of air-cured microconcretes indicates that electrical conductivity (or resistivity) can be used as a rapid and non-destructive method for prediction of chloride ion permeability, independently of mixture's binder composition.
- The higher the volume of pozzolanic materials like Metakaolin and Fly Ash in the binder, the higher the carbonation of the microconcrete, due to the low available amount of $Ca(OH)_2$ in the matrix.

REFERENCES

[1] Hassan, K.E., J.G. Cabrera, and R.S. Maliehe, *The effect of mineral admixtures on the properties of high-performance concrete.* Cement and Concrete Composites, 2000. **22**(4): p. 267-271.
[2] Basheer, P.A.M., S.E. Chidiact, and A.E. Long, *Predictive models for deterioration of concrete structures.* Construction and Building Materials, 1996. **10**(1): p. 27-37.
[3] Castro, P., O.T. De Rincon, and E.J. Pazini, *Interpretation of chloride profiles from concrete exposed to tropical marine environments.* Cement and Concrete Research, 2001. **31**(4): p. 529-537.
[4] Dhinakaran, G., S. Thilgavathi, and J. Venkataramana, *Compressive strength and chloride resistance of metakaolin concrete.* KSCE Journal of Civil Engineering, 2012. **16**(7): p. 1209-1217.
[5] Papadakis, V.G., *Effect of supplementary cementing materials on concrete resistance against carbonation and chloride ingress.* Cement and Concrete Research, 2000. **30**(2): p. 291-299.
[6] Batis, G., et al., *The effect of metakaolin on the corrosion behavior of cement mortars.* Cement and Concrete Composites, 2005. **27**(1): p. 125-130.
[7] Bredy, P., M. Chabannet, and J. Pera, *Microstructure and Porosity of Metakaolin Blended Cements.* MRS Online Proceedings Library, 1988. **137**: p. null-null.
[8] Cabrera, J.G. and S.O. Nwaubani. *The microstructure and chloride ion diffusion characteristics of cements containing metakaolin and fly ash.* in *Sixth CANMET/ACI/JCI International Conference on Fly Ash, Silica Fume, Slag and Natural Pozzolans in Concrete*. 1998. Bangkok, Thailand.
[9] Güneyisi, E., M. Gesoğlu, and K. Mermerdaş, *Improving strength, drying shrinkage, and pore structure of concrete using metakaolin.* Materials and Structures, 2008. **41**(5): p. 937-949.
[10] Poon, C.S., S.C. Kou, and L. Lam, *Compressive strength, chloride diffusivity and pore structure of high performance metakaolin and silica fume concrete.* Construction and Building Materials, 2006. **20**(10): p. 858-865.
[11] J., B., W. S., and G. A., *Accelerating early strength development of concrete using metakaolin as an admixture.* Materials Science (Medziagotyra), 2004. **10**(4): p. 338-344.
[12] Chindaprasirt, P., C. Jaturapitakkul, and T. Sinsiri, *Effect of fly ash fineness on compressive strength and pore size of blended cement paste.* Cement and Concrete Composites, 2005. **27**(4): p. 425-428.
[13] Rassouly, S.M.K., *The packing density of `perfect' binary mixtures.* Powder Technology, 1999. **103**(2): p. 145-150.
[14] Aiqin, W., Z. Chengzhi, and Z. Ningsheng, *The theoretic analysis of the influence of the particle size distribution of cement system on the property of cement.* Cement and Concrete Research, 1999. **29**(11): p. 1721-1726.

[15] Wang, A., C. Zhang, and N. Zhang, *Study of the influence of the particle size distribution on the properties of cement.* Cement and Concrete Research, 1997. **27**(5): p. 685-695.

[16] Binici, H., et al., *The effect of particle size distribution on the properties of blended cements incorporating GGBFS and natural pozzolan (NP).* Powder Technology, 2007. **177**(3): p. 140-147.

[17] Bai, J., et al. *Strength development in concrete incorporating PFA and metakaolin*. Magazine of Concrete Research, 2000. **52**, 153-162.

[18] Bai, J., S. Wild, and B.B. Sabir, *Sorptivity and strength of air-cured and water-cured PC–PFA–MK concrete and the influence of binder composition on carbonation depth.* Cement and Concrete Research, 2002. **32**(11): p. 1813-1821.

[19] Badogiannis, E., et al., *Exploitation of poor Greek kaolins: strength development of metakaolin concrete and evaluation by means of k-value.* Cement and Concrete Research, 2004. **34**(6): p. 1035-1041.

[20] Courard, L., et al., *Durability of mortars modified with metakaolin.* Cement and Concrete Research, 2003. **33**(9): p. 1473-1479.

[21] Al-Akhras, N.M., *Durability of metakaolin concrete to sulfate attack.* Cement and Concrete Research, 2006. **36**(9): p. 1727-1734.

[22] Boddy, A., R.D. Hooton, and K.A. Gruber, *Long-term testing of the chloride-penetration resistance of concrete containing high-reactivity metakaolin.* Cement and Concrete Research, 2001. **31**(5): p. 759-765.

[23] BSI, *BS EN 1008:2002 - Mixing water for concrete. Specification for sampling, testing and assessing the suitability of water, including water recovered from processes in the concrete industry, as mixing water for concrete*. 2002, BSI: EU. p. 22.

[24] Build, N., *492. Concrete, mortar and cement-based repair materials: chloride migration coefficient from non-steady-state migration experiments*, in *Nordtest method*. 1999. p. 10.

[25] Ismail, I., et al., *Influence of fly ash on the water and chloride permeability of alkali-activated slag mortars and concretes.* Construction and Building Materials, 2013. **48**(0): p. 1187-1201.

[26] Celik, K., et al., *High-volume natural volcanic pozzolan and limestone powder as partial replacements for portland cement in self-compacting and sustainable concrete.* Cement and Concrete Composites, 2014. **45**(0): p. 136-147.

[27] Snyder, K.A., et al., *Using Impedance Spectroscopy to Assess the Viability of the Rapid Chloride Test for Determining Concrete Conductivity.* Journal of Research of the National Institute of Standards and Technology, 2000. **105**(4): p. 497-509.

[28] Lizarazo-Marriaga, J. and P. Claisse, *Determination of the concrete chloride diffusion coefficient based on an electrochemical test and an optimization model.* Materials Chemistry and Physics, 2009. **117**(2–3): p. 536-543.

[29] McCarter, W.J., G. Starrs, and T.M. Chrisp, *Electrical conductivity, diffusion, and permeability of Portland cement-based mortars.* Cement and Concrete Research, 2000. **30**(9): p. 1395-1400.

[30] Lu, X., *Application of the Nernst-Einstein equation to concrete.* Cement and Concrete Research, 1997. **27**(2): p. 293-302.

[31] BSI, *BS 1881-201:1986 - Testing concrete Guide to the use of non-destructive methods of test for hardened concrete*. 1986, BSI: UK. p. 26.